ISBN: 978-3-95450-132-8 doi:10.18429/JACoW-IPAC2014-MOPRO054

COMMISSIONING PROGRESS OF THE FEMTOSLICING AT SOLEIL

M. Labat, M.-A. Tordeux, P. Hollander, P. Prigent, M.-E. Couprie, A. Nadji, D. Pédeau, J.-P. Ricaud, F. Dohou, L. Cassinari, O. Marcouillé, H. Abualrob, K. Tavakoli, D. Zerbib, J.-L. Marlats, A. Lestrade, M. Ros, L. Nadolski, J.-F. Lamarre, P. Betinelli, A. Buteau, N. Béchu, C. Herbeaux, P. Roy, J. Luning, T. Moreno, C. Laulhe, S. Ravy, M. Silly, F. Sirotti, P. Morin, Synchrotron SOLEIL, L'Orme des Merisiers, 91 191 Gif-sur-Yvette, France

Abstract

The femtoslicing project at SOLEIL is currently under commissioning. It will enable to serve several beamlines with 100 fs FWHM long pulses of soft and hard X-rays with reasonable flux and with a 1 kHz repetition rate. It is based on the interaction of a femtosecond Ti:Sa laser with electrons circulating in the magnetic field of a modulator wiggler, that provides the electron beam energy modulation on the length scale of the laser pulse. The optimization of the interaction is performed using two dedicated diagnostics stations. The first one, operating in the Infra-Red (IR) is installed in the tunnel and allows the adjustment of the temporal, spectral and spatial overlap between the laser and the electron beam. The second one, located in the IR-THz AILES beamline, measures the intensity of the terahertz (THz) radiation emitted by the local dip structure produced in the core electron beam after interaction. This second setup provides refined optimization of the interaction. This paper describes the layout of these diagnostics and gives first results and characterization of the slicing experiment at SOLEIL.

INTRODUCTION

Third generation synchrotron light sources deliver bright pulses in the soft and hard X-rays domain with a typical duration of a few tens of picoseconds. At SOLEIL, during a few weeks per year, shorter pulses of a few ps are possible thanks to the low-alpha operation mode [1]. Nevertheless part of some user's experiments aim at time resolved measurements at even shorter timescales. Since a few years, several techniques could be implemented on storage rings to reduce further the pulse duration, among which the so-called femtoslicing [2]. A short pulse duration infra-red laser co-propagates with a relativistic electron beam inside the magnetic field of a wiggler, referred from now on as "modulator". The interaction between the laser electric field and the electrons leads to an energy modulation of the electron beam at the length scale of the laser, i.e. over a few tens of femtoseconds typically. At the exit of the modulator, the electron beam is sent through dispersive elements which enable to separate, thanks to their energy offset, the electrons in the short area which has interacted with the laser from the core beam. Transported to a bending magnet or an undulator, the resulting two slices (from positive and negative energy offset) can deliver synchrotron pulses of a few tens of femtoseconds duration.

Femtoslicing is in operation at ALS [3], BESSY-II [4] and SLS [5]. The commissioning at SOLEIL started in January 2014 with dedicated machine time on Mondays when the laser is available.

SOLEIL FEMTOSLICING SCHEME

The SOLEIL femtoslicing scheme differs slightly from the three mentioned above. (1) The laser is used both for the electron beam modulation and as a pump for pump-probe experiments for the two first beamlines which will use the femtoslicing. This laser can deliver 800 nm pulses of 5 mJ at 1 kHz with 30 to 1 000 fs-FWHM duration. It belongs to the CRISTAL beamline [6]. (2) The wiggler used as modulator will serve as a synchrotron radiation source for the forthcoming PUMA beamline. This wiggler has 20 periods of 164.4 mm with a maximum magnetic field of 1.81 T [7]. (3) The separation method exploits the non-zero horizontal dispersion in the straight sections of SOLEIL while other machines use dedicated dipoles. Figure 1 illustrates the trajectory experienced by the slice with an energy offset of 20 MeV, which is above 7 times the natural beam energy spread of 10^{-3} at full energy, 2.75 GeV.

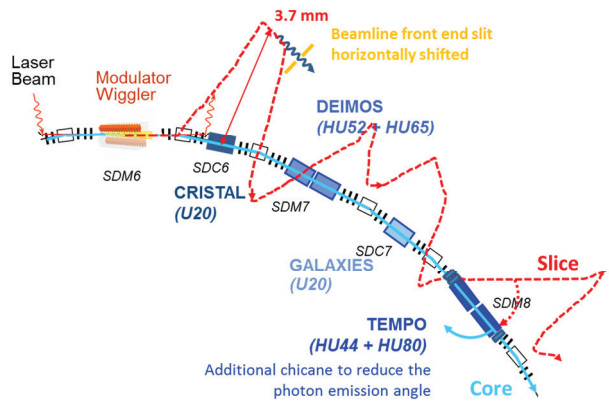

Figure 1: Horizontal plane trajectory experienced by the 20 MeV energy offset satellite (red dashed line) and the beam core (cyan line).

(4) The last specificity is the number of users expected, thanks to moderate slice lengthening throughout the successive dipoles along the ring. Phase 1 foresees two user beamlines: CRISTAL (hard X-rays) and TEMPO (soft X-rays). The CRISTAL frontend entrance slit is now modified to intercept either the horizontally shifted slice

ISBN: 978-3-95450-132-8 doi:10.18429/JACoW-IPAC2014-MOPRO054

or the main centred beam. An additional electromagnetic chicane is under design for the TEMPO straight section to steer the sliced beam undulator radiation right to the centre of the first mirror of the beamline. Moreover, three other beamlines are interested and their setups are under study: DEIMOS, SEXTANTS (soft X-rays) and GALAXIES (hard X-rays).

MODELING

The interaction between the laser and the electron beam inside the wiggler has been simulated using various codes and different methods. We started using A. Zholents' 1D analytical formula [8]. We then used GENESIS [9] code which enabled us to get a 6D description of the electron beam together with a 1D description of the laser. Finally, we used ELEGANT [10] code for the interaction (6D description of the electron beam and 3D description of the laser) in association with the Accelerator Toolbox AT [11] code for the electron beam transport from the modulator to each users' source point and the tracking over several turns, taking into account the sextupole contribution. The three codes were found in reasonable agreement and enabled us to predict that a mean energy exchange of 20 MeV, compatible with the user beamline acceptances, could be reached with a pulse energy below 1.5 mJ. Figure 2 shows an example of laser parameter optimization maximizing the number of efficient sliced electrons for the CRISTAL beamline.

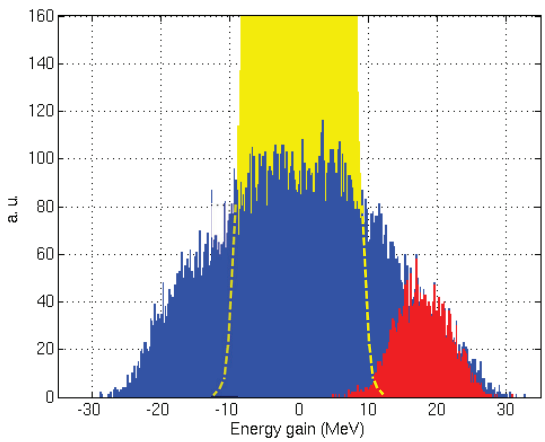

Figure 2: Energy distribution of the electron beam resulting from the interaction (ELEGANT) and 6D tracking (AT code): (yellow) electrons from the core beam, (blue) electrons from the positive and negative energy offset slices, (red) efficient electrons for the CRISTAL beamline with a diaphragm located at s=17 m from its source point and x=+2.7 mm from its 0° axis in the frontend.

The expected performances on the various beamlines have also been simulated. Considering the whole slice with electrons having a positive energy offset above 8 MeV and assuming a 35 fs-FWHM laser pulse (50 fs electric field), the expected pulse durations on the various beamlines are: 125 fs-FWHM at CRISTAL, a reduced duration of 65 fs-FWHM at DEIMOS by a sextupolar effect, and 180 fs-FWHM at TEMPO. Using the 6D electron beam distribution at the CRISTAL undulator entrance, further calculations were done by ray tracing using the code SpotX [12].

Then, taking into account the optimization of the frontend slit horizontal position at x=+2.7 mm and the monochromator selection, a photon flux of 5.10^5 ph/s can be expected at 7 keV with an X-ray pulse duration of 90 fs-FWHM.

SOLEIL LAYOUT

The general layout for the femtoslicing experiment is illustrated in figure 3. The laser hutch is located in CRISTAL beamline. The laser is transported over a distance of ~80 m under 0.1 mbar pressure into the ring tunnel and injected for co-propagation on the electron beam axis inside the wiggler vacuum chamber. In the tunnel, a lens of 9 m focal length focusses the beam in the middle of the wiggler. The alignment of the laser from its hutch down to the wiggler, with a precision of a few tens of µm /µrad in the last straight section in the wiggler, revealed much more difficulties than expected.

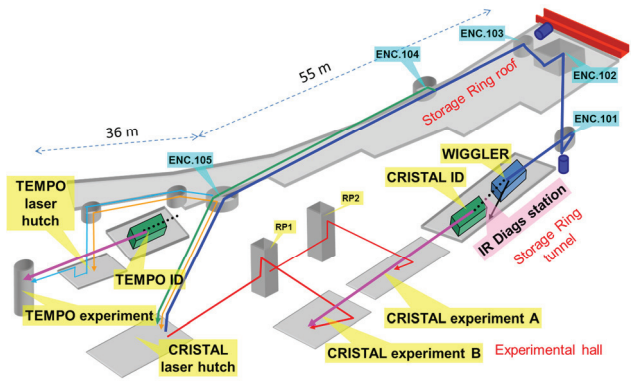

Figure 3: Femtoslicing layout at SOLEIL. Laser path: (dark blue) from laser hutch to wiggler, (green) back from the roof to laser hutch, (red) from hutch to CRISTAL beamline for pump use, (orange) from laser hutch to TEMPO beamline for synchronization purposes, (light blue) back from the roof to the TEMPO beamline for pump use.

DIAGNOSTICS

IR Diagnostics

At the exit of the wiggler, the laser beam and the synchrotron radiation produced in the wiggler, propagate straight forward down to the PUMA frontend. Just at the entrance of this frontend, a removable copper mirror is installed, enabling the extraction of the two beams, provided the electron beam current is below 10 mA. The beams are then transported to a breadboard installed inside the tunnel under the PUMA frontend. This breadboard is equipped with three types of detectors. A fast photodiode enables us to visualize the delay between

ISBN: 978-3-95450-132-8 doi:10.18429/JACoW-IPAC2014-MOPRO054

the arrival time of the laser and the electron beam inside the wiggler in order to synchronize the laser with the electron beam with a precision of a ~10 ps. A spectrometer measures both radiation spectra so that the wiggler gap can be adjusted to match the laser central wavelength. Finally a CCD camera on a translation stage images both beams inside the wiggler at +/- 1.5 m around the wiggler centre, which enables to adjust the spatial alignment of the laser on the electron beam. Figure 4 shows first acquisition of both beam images.

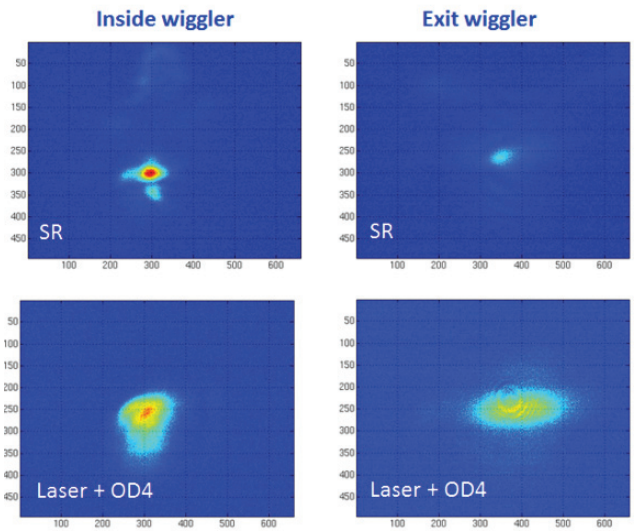

Figure 4: CCD images of the synchrotron radiation (4 mA electron beam current) and of the laser (0.2 W) at two locations inside the wiggler closed at 16.7 mm gap. OD = Optical Density.

THz Diagnostics

After laser and electron beam interaction in the wiggler and propagation along the dispersive optics, the electron beam is left with a depletion area in its centre of duration ~100 fs-FWHM, i.e. 0.03 mm. It will produce coherent THz radiation in any bending magnet. And since the more efficient is the interaction, the more pronounced is this depleted structure, the THz signal intensity will be used to optimize the interaction. At SOLEIL, this THz radiation is collected at the IR-THz AILES beamline, using a removable mirror in one of AILES spectrometers, and transported to either a bolometer or a THz fast diode. The bolometer (from QMC) has a long time response of ~1 ms, but a high sensitivity (1.5 10^{-12} W/sqrt(Hz)). The THz diode (from Virginia Diodes) has a short time response of ~1 ns but a low sensitivity. Both detectors have been tested at SOLEIL in single bunch mode (figure 5). At low current (below 7 mA), the single bunch emits incoherent THz radiation with an intensity proportional to the beam current. The bolometer is sensitive enough to detect this radiation, which is not the case for the diode. At high current (over 8 mA), the single bunch becomes unstable and produces bursts of coherent THz radiation, more intense by at least two orders of magnitude than the incoherent radiation. Both detectors can record this radiation but only the diode can resolve its time structure. Consequently, the bolometer is planned to be used to detect first signature of interaction and further optimization. The diode is planned to be used for more refined dynamical studies of the femtoslicing.

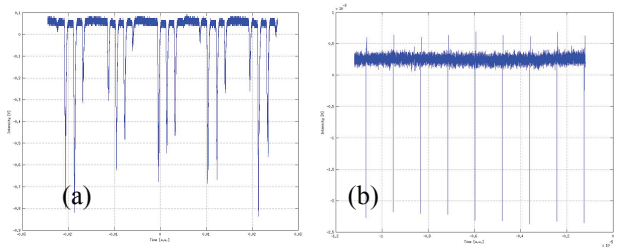

Figure 5: Intensity of the coherent THz signal vs time measured in single bunch mode at high current at SOLEIL. (a) Bolometer signal with a current of 13 mA, the modulation is produced by a chopper for acquisition in AC mode; peaks correspond to ms duration bursts. (b) Diode signal with a current of 13.7 mA, peaks correspond to turn-by-turn emission.

CONCLUSION

The installation of the femtoslicing experiment was completed at the end of 2013. Since January 2014, the commissioning is proceeding. The laser fine alignment throughout the long transport line down to the wiggler is a challenging task. Nevertheless, thanks to some recent improvements in the alignment procedure and in the imaging method inside the wiggler, we expect to demonstrate a first interaction by summer 2014.

REFERENCES

[1] M.-A. Tordeux et al., Proc. of IPAC'2012, 1608-1610.
[2] A. Zholents, M. S. Zoloterev, Phys. Rev. Lett. 76, 912 (1996).
[3] W. Schoenlein et al., Science 287 (2000), 2237.
[4] K. Holldack et al., Phys. Rev. Lett. 96, 054801 (2006).
[5] A. Streun et al., Proc. Of the EPAC'2006 Conference, Edinburgh, Scotland, 3427-3429 (2006).
[6] P. Prigent et al., these Proc.
[7] O. Marcouillé et al., these Proc.
[8] A. A. Zholents, Proc. of PAC'07, 69-73 (2007).
[9] S. Reiche, NIM A 429, 243 (1999).
[10] M. Borland, Proc. of ICAP2000, LS-287 (2000).
[11] A. Terebilo. Accelerator toolbox for MATLAB, Technical Report SLACPUB-8732, Stanford Linear Accelerator Center, May 2001.
[12] T. Moreno and al., J. Phys. IV France 11, 527–531 (2001).